

## Evaluation of Deformation Behavior of a Natural Slope Using Particle Filter

Toshifumi Shibata<sup>1</sup>, Shin-ichi Nishimura<sup>2</sup>, and Takayuki Shuku<sup>3</sup>

<sup>1</sup>Graduate School of Environmental and Life Science, Okayama University,  
3-1-1 Tsushima-Naka, Kita-ku, Okayama 700-8530, Japan.

E-mail: tshibata@cc.okayama-u.ac.jp

<sup>2</sup>Graduate School of Environmental and Life Science, Okayama University,  
3-1-1 Tsushima-Naka, Kita-ku, Okayama 700-8530, Japan.

E-mail: theg1786@cc.okayama-u.ac.jp

<sup>3</sup>Graduate School of Environmental and Life Science, Okayama University,  
3-1-1 Tsushima-Naka, Kita-ku, Okayama 700-8530, Japan.

E-mail: shuku@cc.okayama-u.ac.jp

**Abstract:** This paper shows an evaluation method for landslide behavior using an elasto-viscoplastic finite element (FE) analysis and the particle filter (PF). As the elasto-viscoplastic constitutive model, the Mohr-Coulomb yield criterion with the over-stress model is adopted, and landslide displacements are simulated. The geotechnical parameters related to the creep behavior of a landslide are identified with the PF in this research. The results of the FE analysis using the identified parameters agree well with the observed data, and it is confirmed that the methodology presented in this study can be effective in the evaluation of landslides. In addition, countermeasures for landslides are discussed based on the predicted displacements; and consequently, the possibility of the proposed method's practical use is verified for the mitigation of landslide hazards.

Keywords: Landslides, Displacement prediction, Elasto-viscoplastic analysis, Particle filter

### 1 Introduction

Evaluating the stability of a landslide-prone slope and the ground behavior is crucial in maintenance works (Futatsugi, et al. 2018). The stability of a slope is generally evaluated by the safety factor based on the limit equilibrium method. The method firstly assumes the slip surface using measurements, such as those taken by inclinometers, and strain data. Then, the strength parameters, such as the angle of internal friction and cohesion along the slip surface, are determined from the measurements to perform the stability analysis. As several undisturbed samples close to the slip surface are required for a reliable determination of the strength parameters, difficulties are encountered in the application of soil investigations due to budget limitations. In order to solve these difficulties, the  $c$ - $\tan\phi$  diagram, assuming a certain safety factor, is alternatively used for the determination. However, the mechanical evidence for the experimental determination using the diagram is often inadequate for discussing the real behavior of landslides.

To monitor landslide behavior, inclinometers, extensometers, pipe strain gauges, and water level gauges are generally installed at the actual landslide site. The observation data are used to evaluate the scale and range of the landslide, to elucidate the mechanism, and to predict the collapse time. However, few works have examined the implementation of countermeasures and accurate predictions that are based purely on a rational interpretation of the measured data applied at the design stage. In order to logically assist in the design of effective technical countermeasures based on the field measurements, the application of inverse analyses using measurements is desirable for the calibration of numerical models by means of the identification of parameters.

This paper presents an evaluation method for landslide behavior using an elasto-viscoplastic finite element (FE) analysis, in which the strength parameters are identified by an inverse analysis based on field measurements. A two-dimensional finite element method, incorporated with the Mohr-Coulomb yield criterion, is carried out to explain the behavior of the landslide, and the parameters are identified by the particle filter. A prediction of the landslide is performed and the effects of countermeasures for landslides are numerically investigated.

### 2 Analysis

#### 2.1 Elasto-viscoplastic finite element method

Herein, the elasto-viscoplastic finite element method (Zienkiewicz and Corneau 1974) is briefly described. It is firstly assumed that the total strain rate is divided into elastic and viscoplastic components.

$$\dot{\epsilon}_{ij} = \dot{\epsilon}_{ij}^e + \dot{\epsilon}_{ij}^{vp} \quad (1)$$

where  $\dot{\epsilon}_{ij}$  is the total strain rate tensor,  $\dot{\epsilon}_{ij}^e$  is the elastic strain rate tensor, and  $\dot{\epsilon}_{ij}^{vp}$  is the viscoplastic strain rate tensor. The total stress rate is related to the elastic strain rate as

$$\dot{\sigma}_{kl} = D_{ijkl} \dot{\epsilon}_{ij}^e \tag{2}$$

where  $\dot{\sigma}_{kl}$  is the total stress rate and  $D_{ijkl}$  is the elasticity tensor. The following well-known Mohr-Coulomb yield criterion is adopted as the yield function:

$$F = (\sigma'_1 - \sigma'_3) / 2 - c' \cos \phi' - (\sigma'_1 + \sigma'_3) \sin \phi' \tag{3}$$

where  $F$  is the yield function,  $\sigma'_1$  is the major principal stress,  $\sigma'_3$  is the minor principal stress,  $c'$  is the effective cohesion, and  $\phi'$  is the effective internal angle of friction. The viscoplastic flow rule for an overstress type of elasto-viscoplastic constitutive model (Owen and Hinton 1980) is generally expressed as

$$\dot{\epsilon}_{ij}^{vp} = \gamma \langle \Phi(F) \rangle \frac{\partial Q}{\partial \sigma_{ij}} \tag{4}$$

where  $Q$  is the plastic potential,  $\gamma$  is the fluidity parameter, and  $\Phi$  is the function of overstress. In this paper, the plastic potential is determined by the following equation:

$$Q = (\sigma'_1 - \sigma'_3) / 2 - (\sigma'_1 + \sigma'_3) \sin \Psi + k \tag{5}$$

where  $\Psi$  is the dilatancy angle and  $k$  is the constant parameter. The function of overstress is the monotone increasing function in terms of  $F > 0$ , and the angle brackets mean

$$\begin{aligned} \langle \Phi(F) \rangle &= \Phi(F) \quad F > 0 \\ \langle \Phi(F) \rangle &= 0 \quad F \leq 0 \end{aligned} \tag{6}$$

The function of overstress is expressed as

$$\Phi(F) = F \tag{7}$$

### 2.2 Particle filter

The particle filter (henceforth, PF) (Gordon et al. 1993; Kitagawa 1996) is one of the inverse analysis techniques. The PF can easily deal with nonlinear and non-Gaussian estimation problems, and is robust when employing the Monte Carlo method in conjunction with a numerical simulation. The PF considers the probabilistic density function of a state  $x_t$ , and the function is approximated by an ensemble consisting of a large number of discrete samples which are called particles or samples. A filtered distribution at time  $t-1$ ,  $p(x_{t-1} | y_{1:t-1})$ , is expressed by particles  $\{x_{t-1|t-1}^{(1)}, x_{t-1|t-1}^{(2)}, \dots, x_{t-1|t-1}^{(N)}\}$  and weights  $\{w_{t-1}^{(1)}, w_{t-1}^{(2)}, \dots, w_{t-1}^{(N)}\}$  as

$$p(x_{t-1} | y_{1:t-1}) \approx \sum_{i=1}^N w_{t-1}^{(i)} \delta(x_{t-1} - x_{t-1|t-1}^{(i)}) \tag{8}$$

where  $\delta$  is Dirac's delta function and  $N$  is the number of particles in the ensemble.  $y_{1:t-1}$  means the set  $\{y_1, y_2, \dots, y_{t-1}\}$ . An ensemble approximation of the predicted distribution  $p(x_t | y_{1:t-1})$  at the next observation time  $t$  is given from this ensemble and weights as

$$p(x_t | y_{1:t-1}) \approx \sum_{i=1}^N w_{t-1}^{(i)} \delta(x_t - x_{t|t-1}^{(i)}) \tag{9}$$

From the predicted distribution  $p(x_t | y_{1:t-1})$  and observation  $y_t$ , a filtered probabilistic density function  $p(x_t | y_{1:t})$  using Bayes' theorem is expressed as follows:

$$p(x_t | y_{1:t}) = \sum_{i=1}^N w_t^{(i)} \delta(x_t - x_{t|t-1}^{(i)}) \tag{10}$$

where weight  $w_t^{(i)}$  is defined as

$$w_t^{(i)} = \frac{p\left(y_t \mid x_{t-1}^{(i)}\right)}{\sum_j p\left(y_t \mid x_{t-1}^{(j)}\right)} \tag{11}$$

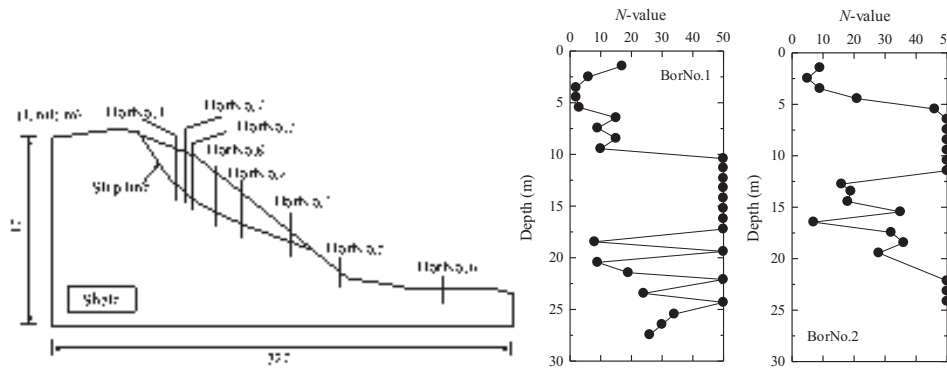
where  $p\left(y_t \mid x_{t-1}^{(i)}\right)$  is the likelihood of  $x_{t-1}^{(i)}$  given data  $y_t$ .

Eq. (10) shows that  $p\left(x_t \mid y_{1:t}\right)$  is approximated based on particles weighted by  $w_t^{(i)}$ . A new ensemble  $\left\{x_{t-1|t-1}^{(1)}, x_{t-1|t-1}^{(2)}, \dots, x_{t-1|t-1}^{(N)}\right\}$ , with a weight of  $w_t^{(i)}$  for each  $i$ , is obtained by Eq. (10). This paper adopts Sequential Importance Sampling (SIS) (Doucet et al. 2000), since it is much more advantageous for nonlinear state equations, such as elasto-viscoplastic problems, than other PF methods.

### 3 Slope analysis for landslide site

#### 3.1 Landslide site

Figure 1 (a) presents a side view of the target slope and eight borehole locations (BorNo.1 – BorNo.8) with the slip line. A landslide with a width of 140 m, a length of 180 m, and a maximum depth of 40 m was caused, and the inclination angle of the slope was almost 40°. Only the data from the standard penetration tests conducted at BorNo.1 and BorNo.2 are given in Fig. 1(b). It should be noted that when the N-value exceeds 50, the value is always set to be 50. Since there is a large variation in N-values beneath the hard strata in Fig. 1 (b), it is implied that a fracture zone due to the landslide lies there. The model consists of three strata, namely, surface strata with an N-value of almost 10, middle strata as the fracture zone, and shale with an N-value over 50.



(a) Section of slip surface at studied site. (b) Distribution of N-values in vertical direction.

Figure 1. Details of target site.

Figure 2 indicates two observed displacements for each of the three strata, namely, the surface, middle strata, and slip line, because only two observation points of displacements were available, namely, BorNo.2 and BorNo.4. The point in the middle strata is located between the surface and the slip line. Only the displacement at BorNo.4 is used in the computation, since continuous measurement was successfully achieved at this point.

#### 3.2 Numerical model

Figure 3 (a) depicts the adopted finite element mesh, consisting of 515 four-node isoparametric quadrilateral elements, and the boundary conditions. Thin elements are located as the fracture zone based on the geotechnical investigations. Figure 3 (b) shows the assignment of the material parameters listed in Table 1, in which “ \* ” indicates the parameters to be identified. Young’s modulus and the angle of internal friction are deduced from the N-values, as follows:

$$E = 2,800N \tag{12}$$

$$\phi = \sqrt{20N} + 15 \tag{13}$$

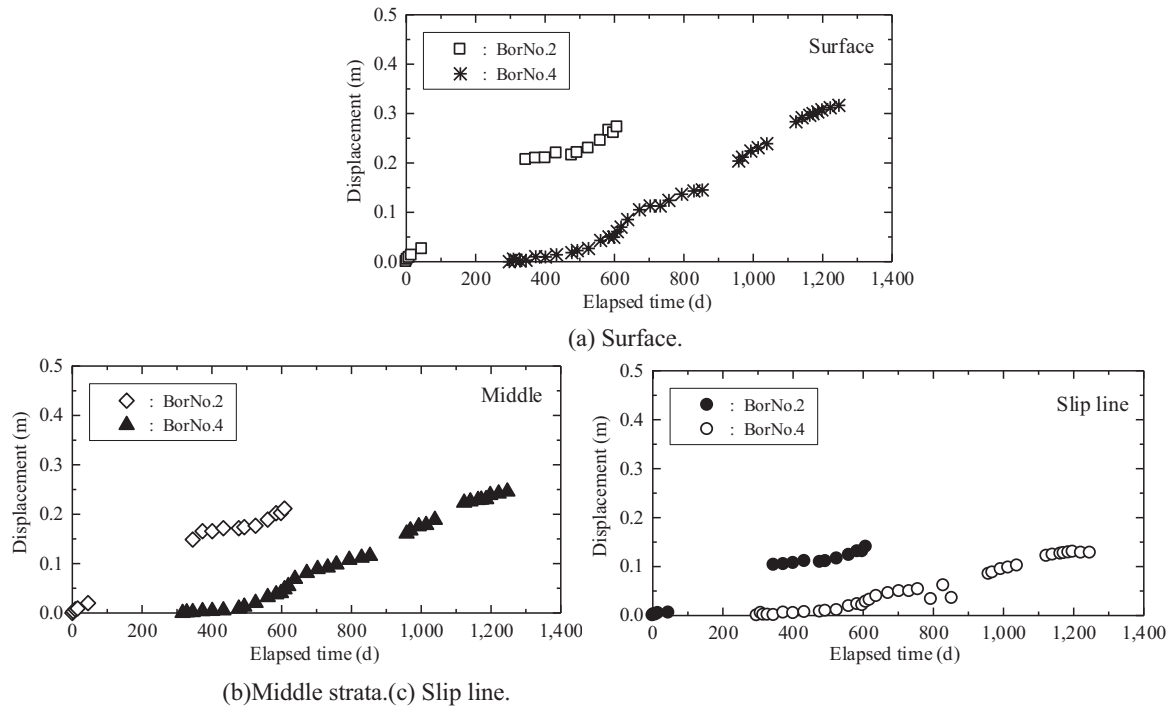


Figure 2. Observed displacements employed in parameter identification.

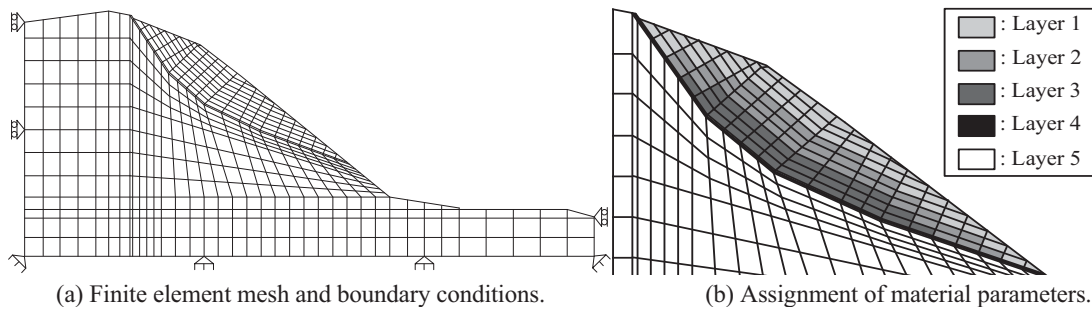


Figure 3. Description of problem for landslide.

The target parameters to be identified are the effective angle of internal friction in Layer 5 and the fluidity parameter, because these two parameters play a primary role in evaluating the creep behavior of landslides. 1,000 simulations are conducted by a Monte Carlo search over the range in parameters listed in Table 2. Each parameter is assumed to follow a uniform distribution and is generated independently. The diagonal term for the observation error covariance matrix,  $R_t$ , is assumed as follows:

$$R_t = \alpha u_i \delta_{ij} \tag{14}$$

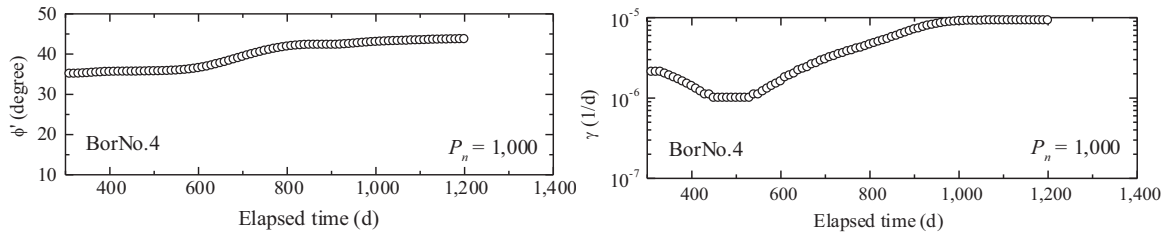
where  $\alpha$  represents the control parameter for the covariance,  $u_i$  is the maximum value at the  $i$ -th observation point, and  $\delta_{ij}$  is Kronecker's delta. The control parameter is chosen as 0.3, and the value is used when successful identification has been achieved (Shuku et al. 2012).

Table 1. Material parameters employed in analyses of studied site.

Layer	N-value	$\gamma_t$ (kN/m <sup>3</sup> )	$E$ (kN/m <sup>2</sup> )	$c'$ (kN/m <sup>2</sup> )	$\phi'$ (degree)	$\gamma$ (1/d)
1	10	18	28,000	0.0	29	*
2	50	22	140,000	0.0	47	*
3	25	20	70,000	0.0	37	*
4	5	20	14,000	0.0	*	*
5	50	23	200,000,000	10,000	0	*

Table 2. Ranges of parameters.

Parameter	Range of particle generation
$\phi'$ (degree)	25.0 ~ 45.0
$\gamma$ (1/d)	$1.0 \times 10^{-7} \sim 1.0 \times 10^{-5}$

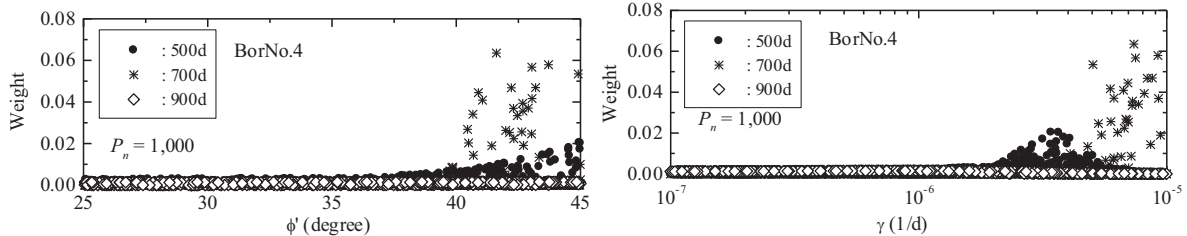


(a) Effective angle of internal friction. (b) Fluidity parameter.

**Figure 4.** Time evolution of identified parameters.

**3.3 Identification of geotechnical parameters**

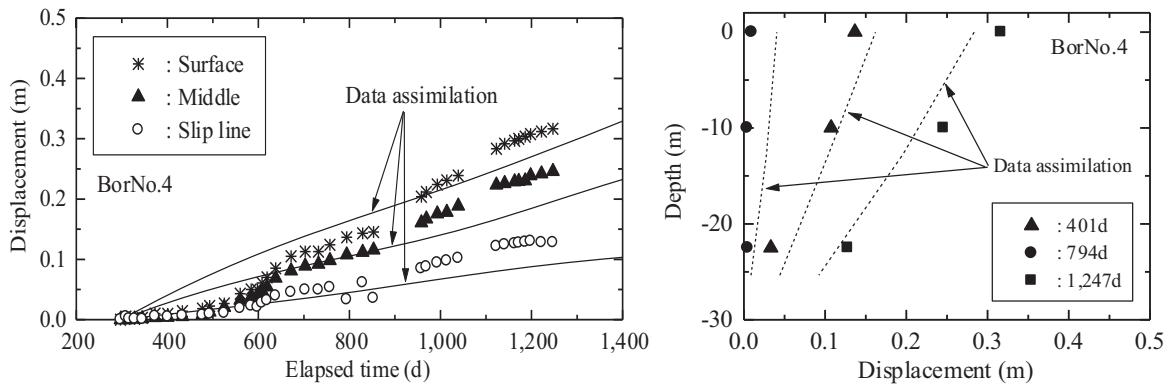
Figure 4 shows the time evolution of the identified parameters, which are obtained by the weighted average of the particles using the computed weight distribution in Eq. (11) at each time. In Fig. 4(a), the effective angle of internal friction stays almost constant before a lapse on the 600th day, then slowly changes along the path occurring after the 600th day, and remains constant with the passage of time after the 800th day. Figure 4 (b) shows the significant changes caused before the 600th day, the identified fluidity parameter moderately increasing up to the 950th day, and then an almost constant value until the 1200th day. Eventually, the effective angle of internal friction and the fluidity parameter indicate  $43.7^\circ$  and  $9.2 \times 10^{-6} \text{ d}^{-1}$ , respectively. Figure 5 depicts the filtered probability density functions of the weight of the identified parameters. The distribution is updated following the measured data.



(a) Effective angle of internal friction. (b) Fluidity parameter.

**Figure 5.** Distribution of weight for each parameter.

Figures 6(a) and (b) compare the observed displacements and the results of the direct analysis using the identified parameters to be described as ‘data assimilation’. Although a small discrepancy appears between the computed results and the observations, a good agreement is shown. The results suggest that the methodology is a highly effective approach for use in geotechnical practice.



(a) Time history of displacements.

(b) Displacements against depth.

**Figure 6.** Results of analysis using identified parameters.

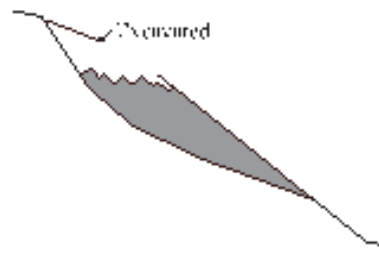
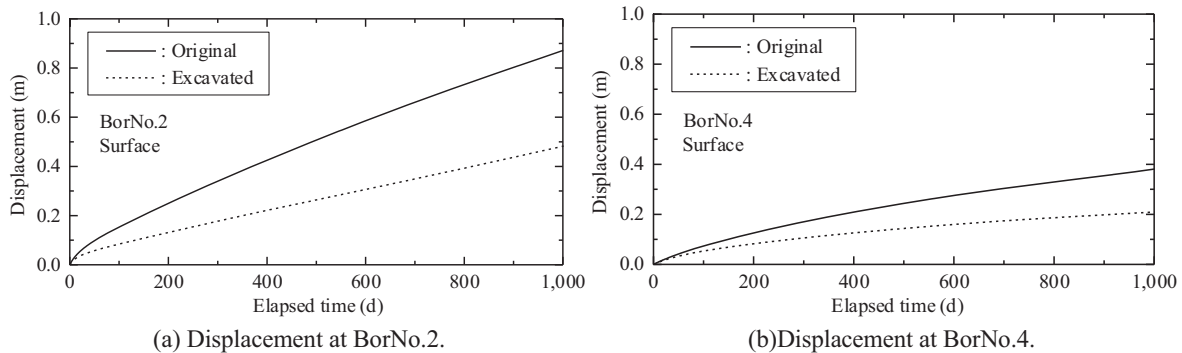


Figure 7. Earth removal work.

### 3.4 Simulation of countermeasures

To discuss the effect of countermeasures for landslides based on the simulated results using the identified parameters, a numerical simulation of the earth removal work is carried out. A direct analysis with the identified parameters, using 0 for the unit weight of the excavated soil, is shown in Fig. 7. Figures 8 (a) and (b) explain the time-displacement relationship of the slope surface with the earth removal work at BorNo.2 and BorNo.4. The broken line is the calculated displacement due to the earth removal work, whereas the solid line indicates the results without any countermeasures. The figures display that the computation can predict the displacement of the landslide and that the removal of soil decreases the displacement. The results verify the potential of the proposed method's practical use for the mitigation of landslide hazards.



(a) Displacement at BorNo.2.

(b) Displacement at BorNo.4.

Figure 8. Time-displacement relationship of slope surface with earth removal work.

## 4 Conclusion

This paper proposed an evaluation method for landslide behavior based on an elasto-viscoplastic finite element (FE) analysis using the identified parameters, namely, the effective angle of internal friction and the fluidity parameter. The particle filter (PF) was employed to identify the geotechnical parameters based on the field measurements. A good match was found between the simulation using the PF approach and the observations. The results imply that the proposed procedure using the PF is an effective method for use in geotechnical practice for predicting landslide hazards.

In order to discuss the effect of countermeasures for landslides, a numerical simulation of earth removal work using the identified parameters was conducted. The results show that the calculation can predict the displacement of a landslide and that the removal of soil decreases the displacement, thus verifying the potential of the proposed method's practical use for the mitigation of landslide hazards.

## References

- Doucet, A., Godsill, S. and Andrieu, C. (2000). On sequential Monte Carlo sampling methods for Bayesian filtering, *Statistics and Computing*, 10, 197-208.
- Futatsugi, S., Nishimura, S., Shuku, T. and Shibata, T. (2018). Evaluation of deformation behavior of a natural slope using elasto-viscoplastic finite element method and observation data, 86(1), *Irrigation, Drainage and Rural Engineering Journal*, II 9-II 18. (in Japanese)
- Gordon, N.J., Salmond, D.J. and Smith, A.F.M. (1993). Novel approach to nonlinear/non-Gaussian Bayesian state estimation, *IEEE Proceedings-F*, 140(2), 107-113.
- Kitagawa, G. (1996). Monte Carlo filter and smoother for non-Gaussian nonlinear state space models, *Journal of Computational Graphical Statistics*, 5(1), 1-25.
- Owen, D.R.J. and Hinton, E. (1980). Finite elements in plasticity: Theory and practice, *Pineridge Press Limited, Swansea*.
- Shuku, T., Murakami, A., Nishimura, S., Fujisawa, K. and Nakamura, K. (2012). Parameter identification for Cam-clay model in partial loading model tests using the particle filter. *Soils and Foundations*. 52 (2), 279-298.
- Zienkiewicz, O.C. and Corneau, I.C. (1974). Visco-plasticity - plasticity and creep in elastic solids - a unified numerical solution approach, *International Journal for Numerical Methods in Engineering*, 8, 821-845.